

# Demonstration for integrating capacitive pressure sensors with read-out circuitry on stainless steel substrate

Sung-Pil Chang\*, Mark G. Allen

*School of Electrical and Computer Engineering, Georgia Institute of Technology, Atlanta, GA 30332-0250, USA*

Received 1 October 2003; received in revised form 30 March 2004; accepted 9 April 2004

Available online 19 May 2004

## Abstract

Capacitive pressure sensors have lots of potential for commercial applications. However, successful commercial exploitation of highly miniaturized capacitive sensors is often inhibited by the presence of parasitic effects such as environmental noise and parasitic capacitances. Therefore, to alleviate the problems encountered in the capacitive pressure sensor approach, it is important to integrate the sensors and the circuitry as directly as possible.

This paper builds on preliminary work reported previously by us [Sens. Actuators A 101 (2002) 231] and focuses on direct integration of read-out circuitry with microfabricated microsensors. These capacitive pressure sensors with three-candidate diaphragm materials (Kapton polyimide film, stainless steel, and titanium) are demonstrated the integration with read-out circuitry on stainless steel substrate. Several approaches for the demonstration of integration have been taken and their various degrees of successes are examined.

As the final stage of this study, a commercially available MS3110 Universal Capacitive Read-out IC from Microsensors Inc. in its un-packaged, die-type was used. This chip in its die-form was integrated via wirebonding to the microfabricated sensors. The sensors that are tested using the IC have only the metal diaphragms of stainless steel. The measured value of relative voltage change is 2.85% over the applied pressure range from 0 to 75 kPa. This sensor contains a gap of 21  $\mu\text{m}$  and has a sensitivity of 0.92 mV/kPa.

© 2004 Elsevier B.V. All rights reserved.

*Keywords:* Capacitive pressure sensor; Robust substrate; Lamination; Micromachining; Integration; Wire bonding

## 1. Introduction

Since the root of micromachining technology is in integrated circuit processing, micromachined devices have been primarily realized using silicon substrates [1–4]. In many applications, these silicon-based devices are then protected mechanically against harsh environments by use of a robust packaging material [5,6]. However, this approach often leads to systems in which the cost of the package equals or exceeds the cost of the micromachined device itself. If this robust packaging material is directly used not only as the packaging or housing, but also as the substrate of the micromachined devices, many of the steps of the packaging process might be reduced, potentially leading to cost savings. Another potential advantage is that due to substrate

robustness, these co-packaged devices may be able to be used in mechanically harsh environments, such as aerospace and oceanography applications.

On the market of MEMS pressure sensors, there are two main types of pressure sensors; one type utilizes capacitive effects in sensing pressure, and the other type uses piezoresistive effects for the same purpose [7]. Much work has been done in both areas, but there is a greater focus on capacitive pressure sensors due to certain advantages that this approach provides. Some of the advantages that it offers over the piezoresistive pressure sensor are higher measurement sensitivity, decreased temperature sensitivity, and reduced power consumption, and better stability [8]. These advantages portend greater potential for commercial applications. However, successful commercial exploitation of these highly miniaturized capacitive sensors is often inhibited by the presence of parasitic effects such as environmental noise and parasitic capacitances. Therefore, to alleviate the problems encountered in the capacitive pressure sensor approach, it is important to integrate the sensors and the circuitry as directly as possible. For example, the

\* Corresponding author. Present address: Optical components and MEMS Lab, Central R&D Institute, Samsung Electro-Mechanics Co., Ltd., 314 Maetan3-Dong, Paldal-Gu, Suwon, Gyunggi-Do 442-743, South Korea. Tel.: +82-312106643; fax: +82-312103515.  
E-mail address: [sp.chang@samsung.com](mailto:sp.chang@samsung.com) (S.-P. Chang).

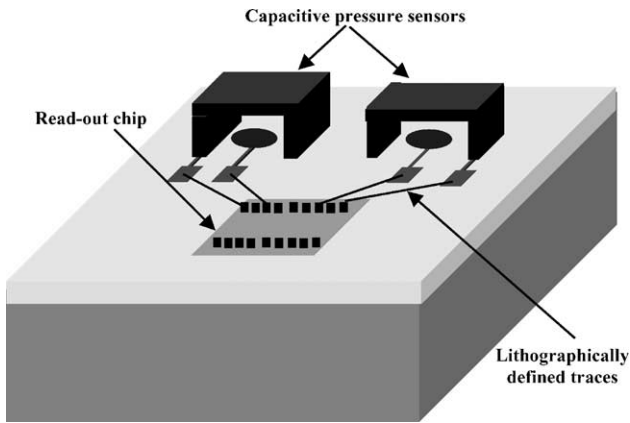


Fig. 1. An example of integrated robust capacitive pressure sensors.

capacitive pressure sensors and the read-out chip are directly integrated on the same substrate by connecting the chip to the sensors using lithographically defined traces as in Fig. 1. This integration allows for buffering and reduction of the parasitic effects as well as the possibility of multiplexing or conversion of capacitances to frequency or voltage.

This study focuses on the effort to directly integrate read-out circuitry with microfabricated sensors. Several approaches have been taken during the course of the research and their various degrees of successes are examined.

## 2. Fabrication process

### 2.1. Fabrication of Kapton diaphragm pressure sensors

The fabrication sequence of the capacitive pressure sensor array is shown in Fig. 2. The process starts on square, stainless steel substrates that are each 5.7 cm on a side, 0.5 mm thick, and have surface roughness of approximately 6–8 μm. An array of 8 × 8 pressure inlet holes with a diameter of 2 mm, with 5 mm center-to-center distances, is milled through the stainless steel substrate. Kapton polyimide film

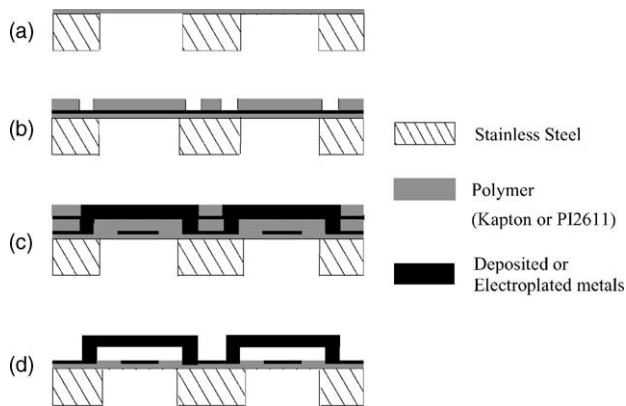
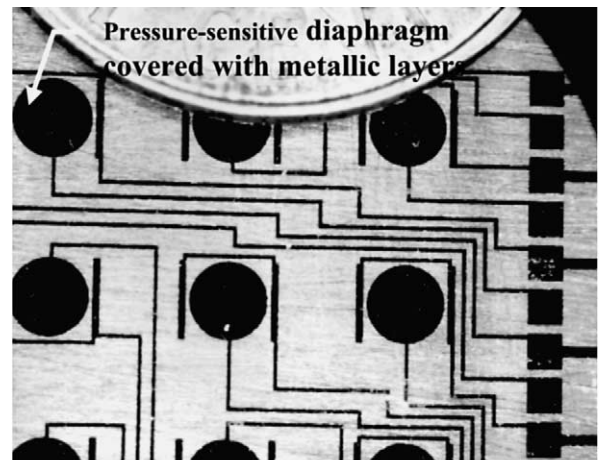


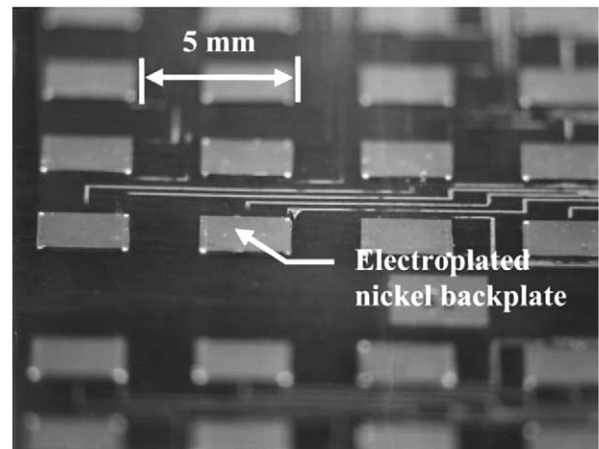
Fig. 2. Fabrication sequence of pressure sensor based on Kapton polyimide diaphragm.

(Dupont, Kapton HN200, 50 μm thick) is laminated onto the milled stainless steel substrate using a hot press with a pressure of 8.65 MPa and a temperature of 175 °C for 30 min. The pressure-sensitive diaphragms will be the Kapton polyimide film in the regions suspended over the milled pressure inlet holes (Fig. 2a).

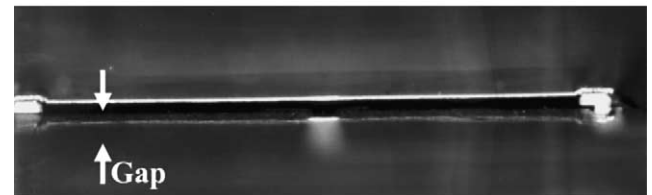
A triple metallic layer of Ti/Cu/Ti with a thickness of 100/2000/500 Å is deposited by electron-beam evaporation and then patterned using a lift-off process to create bottom electrodes, electroplating seed layers, and bonding pads on the surface of the Kapton polyimide film (Fig. 3a). Multiple



(a)



(b)



(c)

Fig. 3. Photographs of fabricated pressure sensor array: (a) a photograph of top-view of the metallic seed layer; (b) a side-view of the pressure sensor array; (c) a close-up view of the gap (approximately 44 μm) defined between electroplated nickel backplate and pressure sensitive Kapton polyimide diaphragm.

layers of PI2611 polyimide (Dupont) are spun onto the patterned layer with a spin speed of 1200 rpm for 60 s, and hard-cured in a  $N_2$  ambient at  $200^\circ C$  for 120 min yielding a final thickness of polyimide of approximately 44–48  $\mu m$ .

The polyimide layer is anisotropically etched using reactive ion etching to create electroplating molds for the support posts of the fixed backplates, and to remove the uppermost titanium layer of the seed layer (Fig. 2b). Nickel supports are then electroplated through the polyimide molds.

A Ti/Cu/Ti metallic triple layer with a thickness of 300/2000/300  $\text{\AA}$  is deposited using DC sputtering to act as a seed layer for the deposition of the backplate. Thick photoresist (Shipley SJR 5740) is spun on the seed layer with a spin speed of 1100 rpm for 30 s (yielding a final thickness of approximately 15  $\mu m$ ) and patterned to act as electroplating molds for the backplates. After removal of the uppermost Ti layer, nickel is electroplated through the thick photoresist electroplating molds to create the backplates (Fig. 2c). The thick photoresist electroplating molds and the remaining seed layer are removed. Finally, the polyimide molds for the backplate posts as well as polyimide sacrificial layers are isotropically etched to create air gaps between the fixed backplates and the pressure sensitive Kapton polyimide flexible diaphragms (Figs. 2d and 3c). The isotropic dry etch is carried out in a barrel plasma etcher using  $CF_4/O_2$  plasma with a RF power of 120 W. Fig. 3 shows photographs of a fabricated pressure sensor array, where (b) shows a side-view and (c) shows a close-up view of the gap defined between the fixed backplate and the diaphragm. Note that these sensors are operating in differential mode, with the side containing the backplate held at a pressure of 1 atm.

### 2.2. Fabrication of stainless steel and titanium diaphragm pressure sensors

The fabrication sequences for the stainless steel diaphragm pressure sensors and the titanium diaphragm

pressure sensors are similar to that of the Kapton diaphragm pressure sensor devices. The same stainless steel substrates and epoxy lamination adhesives as those used in the Kapton diaphragm devices fabrication process are used. Instead of a Kapton polyimide film, a stainless steel sheet (Precision Brand Product Inc.) which has a thickness of 12.7  $\mu m$  and surface roughness of approximately 100  $\text{\AA}$  and a titanium film (Teledyne Rodney Metals, type Ti 540) which has 25.4  $\mu m$  thickness and surface roughness of approximately 60  $\text{\AA}$  are then laminated on the stainless steel substrates, respectively, using a hot press under the same conditions as that of the Kapton diaphragm sensor process.

After lamination of these metal type films, a 7  $\mu m$  thick epoxy resist SU-8-2 (MicroChem Corp.) is spin coated for an insulation layer to isolate the two electrodes. The last processes of this SU-8-2 insulation layer are similar to that of the Kapton diaphragm pressure sensors except for the use of AZ4620 photoresist to form the back post-mold instead of polyimide. Fig. 4 shows the fabricated pressure sensors based on stainless steel diaphragm.

### 3. Capacitance read-out circuitry

Three different stages were undertaken in the development of the read-out circuitry for the capacitance pressure microsensors. The first stage involved the creation of a simple capacitance-to-frequency conversion circuit to directly read the capacitance changes due to applied pressure from the three types of sensors studied in this work: diaphragms of Kapton, stainless steel, and titanium. The second stage involved the use of a commercially available MS3110 Universal Capacitive Read-out IC from Microsensors Inc., along with a supporting MS3110BDPC evaluation board. This board then allowed for the control of the chip by linking it with a PC. The third stage involved the use of the MS3110 IC in its un-packaged, die-form. This chip in its die-form

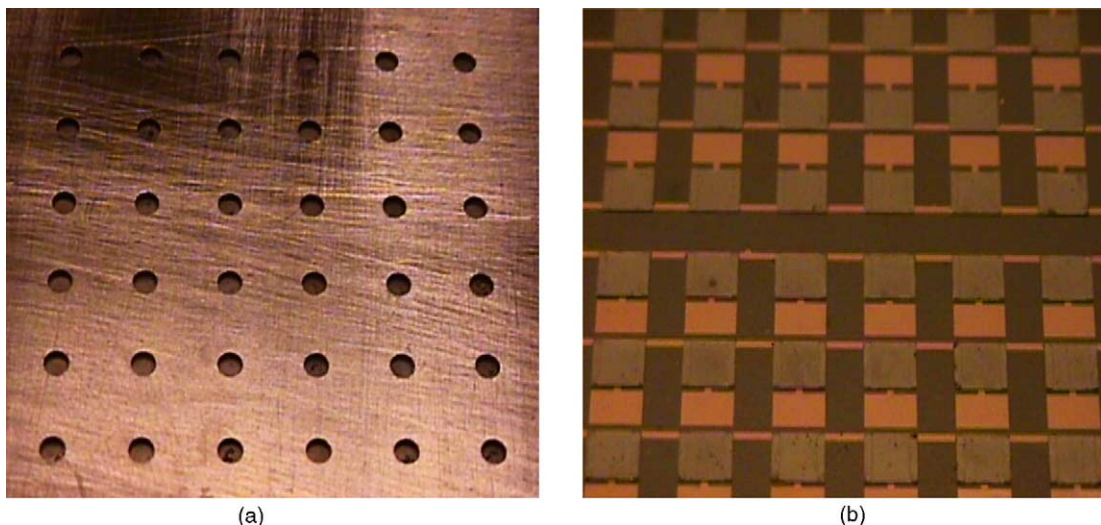


Fig. 4. Photomicrographs of fabricated pressure sensors: (a) side exposed to environment; (b) rear view showing surface micromachined backplate.

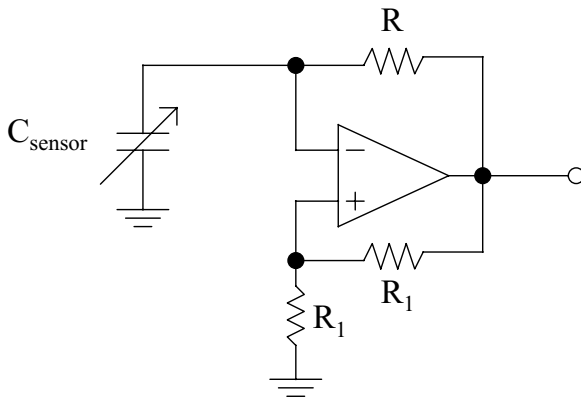


Fig. 5. Schematic diagram of the astable multivibrator circuit.

was then integrated via wirebonding to the microfabricated sensors.

### 3.1. Basic capacitance-to-frequency conversion circuitry

Initially, an op-amp-based astable multivibrator circuit was created in-house to serve as the read-out circuitry for the three types of capacitive pressure sensors. This was then integrated with the pressure sensors in a hybrid fashion to create a frequency-modulated voltage output. Fig. 5 shows a schematic diagram of such an astable multivibrator circuit, which consists of an LF351 operational amplifier, and three external resistors [9].

The capacitance of the pressure sensor is equivalent to the frequency-determining capacitance that modulates the frequency of the voltage output of the amplifier. The output frequency of the op-amp is given by:

$$f = \frac{1}{2RC_{\text{sensor}} \ln 3} \quad (1)$$

where  $RC_{\text{sensor}}$  is the time constant of the circuitry. In this work, external resistors  $R$  and  $R_1$  have been selected as  $1 \text{ M}\Omega$  for all three types of the pressure sensors.

A base frequency of  $12.544 \text{ KHz}$  for the output of the op-amp was found for the Kapton diaphragm pressure sensor. Fig. 6 shows the frequency output of the op-amp circuit as a function of applied pressure from 0 to  $34 \text{ kPa}$  for the Kapton pressure sensor. The measured value of relative frequency change is  $0.93\%$  over the applied pressure range from 0 to  $34 \text{ kPa}$ . This sensor contained a gap of  $40 \mu\text{m}$  and had a sensitivity of  $3.472 \text{ Hz/kPa}$ .

The next sensor-type tested contained the stainless steel diaphragm. For this type of sensor, the base frequency was found to be  $4081.8 \text{ Hz}$  for the output of the op-amp. Fig. 7 shows the frequency output of the op-amp circuit as a function of applied pressure from 0 to  $180 \text{ kPa}$ . The measured value of relative frequency change is  $0.2\%$  over the applied pressure range from 0 to  $180 \text{ kPa}$ . This sensor contained a gap of  $27 \mu\text{m}$  and a sensitivity of  $44.8 \text{ mHz/kPa}$ .

The final sensor-type tested contained the titanium diaphragm. For this type of sensor, the base frequency was found to be  $6037.5 \text{ Hz}$  for the output of the op-amp. Fig. 8 shows the frequency output of the op-amp circuit as a function of applied pressure from 0 to  $182 \text{ kPa}$ . The measured value of relative frequency change is  $0.075\%$  over the applied pressure range from 0 to  $182 \text{ kPa}$ . This sensor contained a gap of  $37 \mu\text{m}$  and a sensitivity of  $24.8 \text{ mHz/kPa}$ .

Fig. 9 shows the experimental test set-up used in evaluating the three types of sensors using the op-amp circuit. For illustrative purposes, the stainless steel diaphragm sensor has been used in the photo. The summarized data of the three types of capacitive pressure sensors with multivibrator circuitry are shown in Table 1.

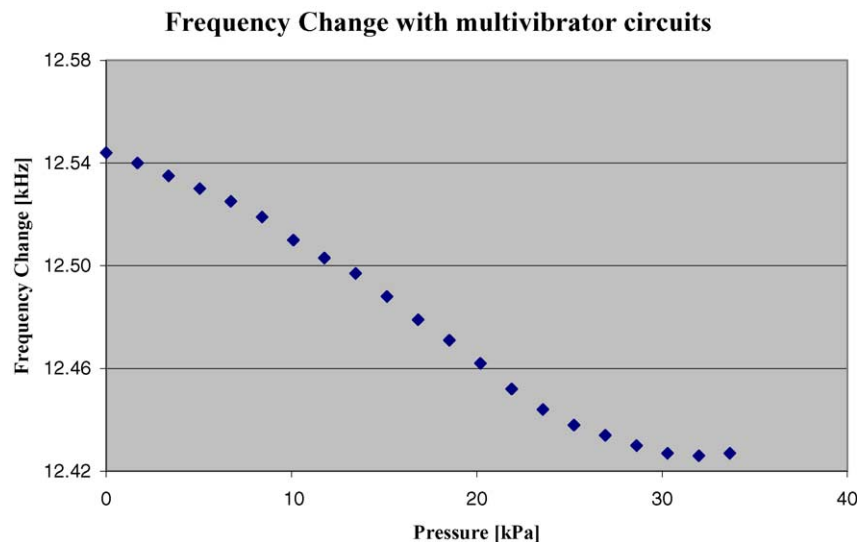


Fig. 6. The frequency output of the op-amp circuit as a function of applied pressure from 0 to  $34 \text{ kPa}$  for the Kapton pressure sensor.



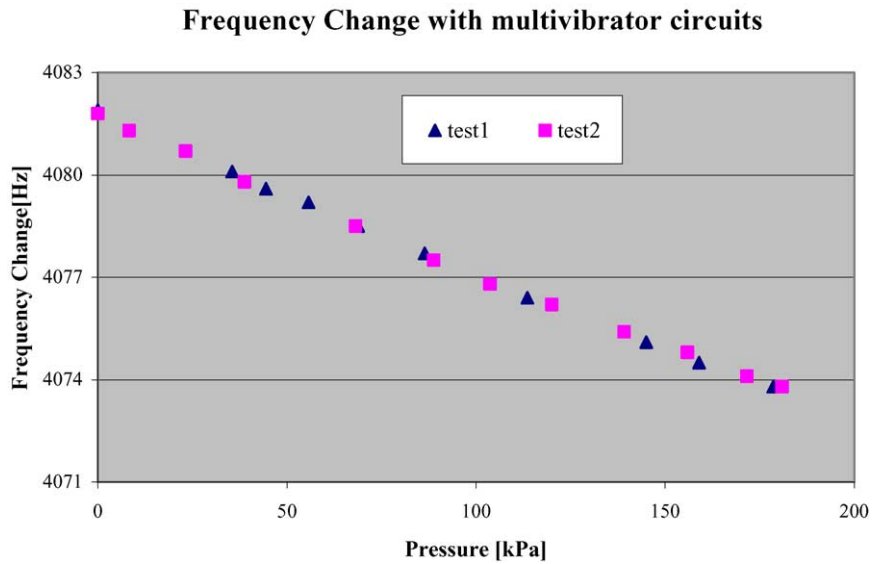


Fig. 7. The frequency output of the op-amp circuit as a function of applied pressure from 0 to 180 kPa for the stainless steel pressure sensor.

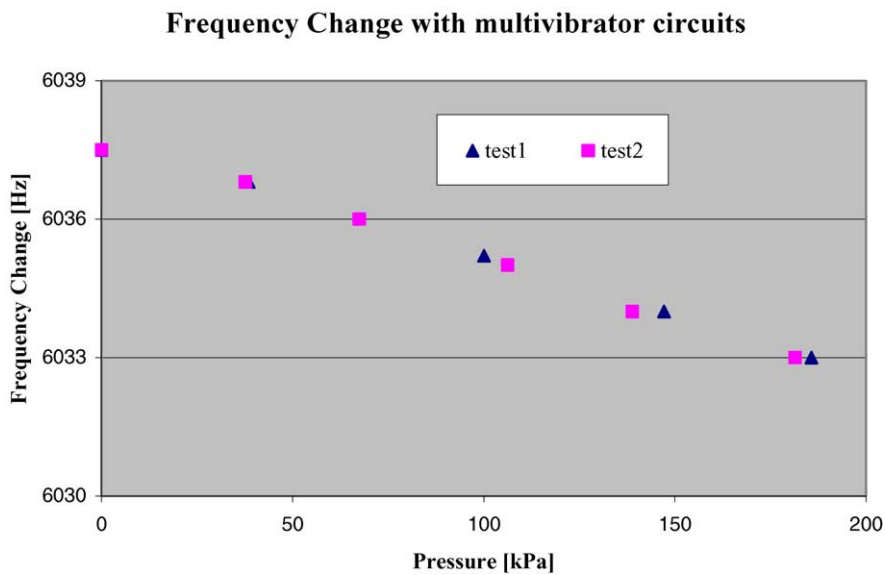


Fig. 8. The frequency output of the op-amp circuit as a function of applied pressure from 0 to 182 kPa for the titanium pressure sensor.

Table 1  
Measured data for three types of capacitive pressure sensors with multivibrator circuitry

	Kapton	Stainless steel	Titanium
Diaphragm radius (mm)	1	1	1
Diaphragm thickness ( $\mu\text{m}$ )	50	12.7	25.4 $\mu\text{m}$
Gap ( $\mu\text{m}$ )	$\approx 40$	$\approx 27$	$\approx 37$
Back plate dimension (mm)	$2.8 \times 2.2$	$3.5 \times 3.0$	$3.5 \times 3.0$
Applied pressure (kPa)	0–34	0–180	0–182
$\Delta f$ (Hz)	117	8.1	4.5
Sensitivity (mHz/kPa)	3.472 <sup>a</sup>	44.8	24.8

<sup>a</sup> In Hz/kPa.

### 3.2. Capacitance-to-voltage conversion circuitry using the MS3110 and MS3110BDPC

The values of capacitance and/or corresponding frequency change produced by the sensors are easily measurable in their current form; however, in order to achieve higher sensitivity, elimination of parasitic capacitance is essential. Primary sources of parasitic capacitance include capacitance between bonding pads and substrates and capacitance between interconnection lines and substrates. Parasitic capacitance from those primary sources can be eliminated by using integrated on-chip circuitry that has a reference electrode, which has the same length of interconnection line and same

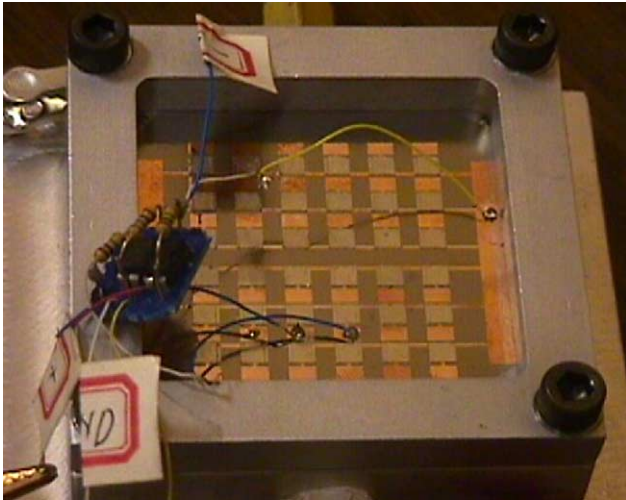


Fig. 9. The experimental test set-up for the stainless steel diaphragm sensor using the op-amp circuit.

structure as that of a pressure sensor with a pressure insensitive (immovable) circular plate.

In order to facilitate the use of this improved on-chip circuitry, a commercially available MS3110 Universal Capacitive Read-out IC was used as the read-out circuit [10]. In the first effort using this IC, a corresponding MS3110BDPC Evaluation Board was used in conjunction with the IC to expedite the testing process. The theory of operation of the MS3110 IC can be summarized by the block diagram below in Fig. 10. The MS3110 senses the difference between two capacitors and outputs a voltage proportional to the difference.

The output voltage can be described by a function of the sensing capacitances  $CS1_T$  and  $CS2_T$ , as shown by the following expression:

$$V_o = \text{Gain} \times V_{2P25} \times 1.14 \times \frac{CS2_T - CS1_T}{CF} + V_{ref} \quad (2)$$

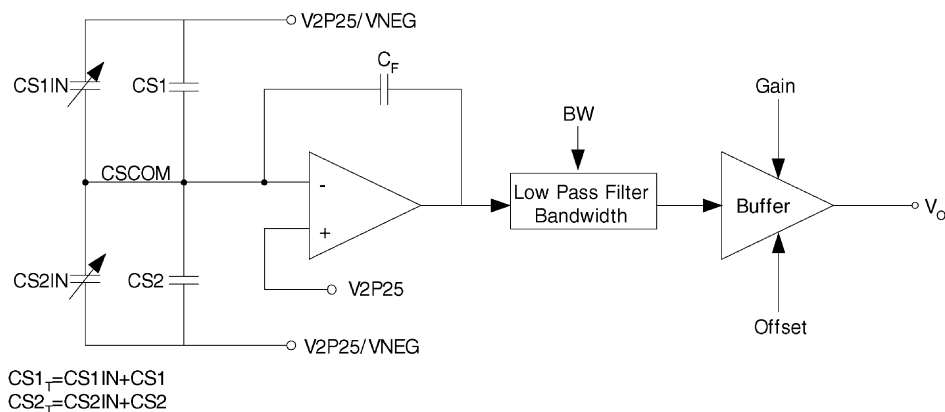


Fig. 10. The block diagram of the MS3110 IC.

$CS2_T$  is the input from the microsensor being tested and  $CS1_T$  is the reference value as input from the reference microsensor. By using the MS3110BDPC Evaluation Board, its ability to program the IC was utilized to find the most favorable parameters under which the IC would function optimally when combined with the microsensors. This information would then be used on stage 3 when the IC would be used in its die-form.

Two types of sensors were tested using the MS3110 IC and the MS3110BDPC. They were sensors with stainless steel and titanium diaphragms. Kapton diaphragm sensors were not tested because Kapton had been used previously in stage 1 to demonstrate the feasibility of robust capacitive pressure sensors using lamination technology combined with microfabrication techniques. Once that had been achieved, the research effort naturally moved on to focus primarily on metal diaphragms. In this case the metals under study were the same two metals of stainless steel and titanium.

Fig. 11 shows the voltage output of the MS3110 for the stainless steel diaphragm sensor, as seen via the MS3110BDPC evaluation board as a function of applied pressure from 0 to 184 kPa. The measured value of relative voltage change is 17.66% over the applied pressure range from 0 to 184 kPa. This sensor contained a gap of 27  $\mu\text{m}$  and a sensitivity of 0.238 mV/kPa.

Fig. 12 shows the voltage output of the MS3110 for the titanium diaphragm sensor, as seen via the MS3110BDPC evaluation board as a function of applied pressure from 0 to 186 kPa. The measured value of relative voltage change is 0.8% over the applied pressure range from 0 to 186 kPa. This sensor contained a gap of 37  $\mu\text{m}$  and a sensitivity of 0.0862 mV/kPa.

Fig. 13 shows the experimental test set-up used in evaluating the sensors using the MS3110 with the MS3110BDPC. For illustrative purposes, the stainless steel diaphragm sensor has been used in the photo.

The summarized data of the two types of capacitive pressure sensors using the MS3110 with the MS3110BDPC are shown in Table 2.

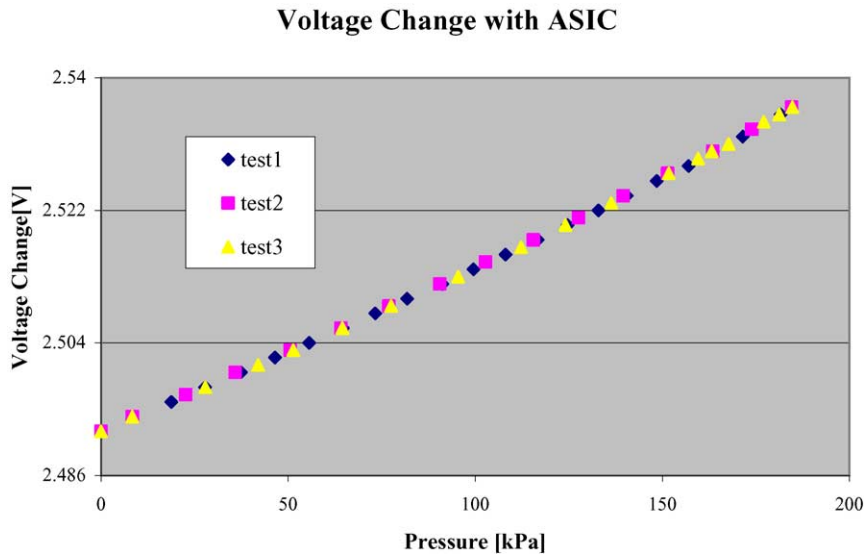


Fig. 11. The voltage output of the MS3110 IC with MS3110BDPC of the sensor with a stainless steel diaphragm.

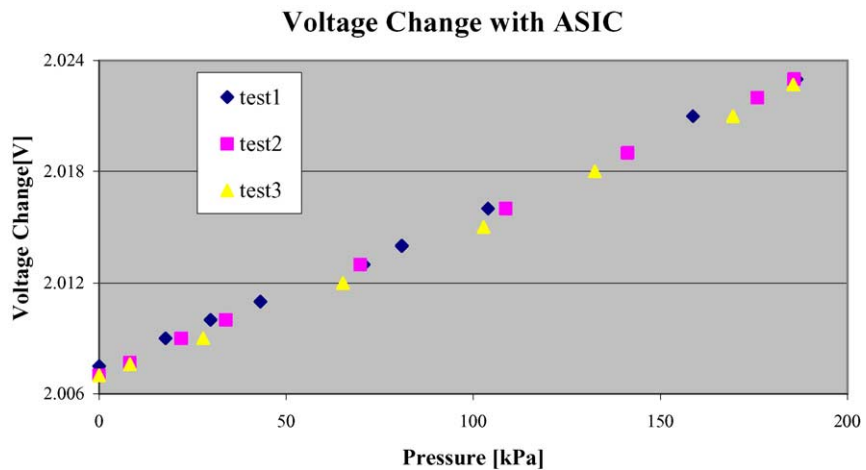


Fig. 12. The voltage output of the MS3110 IC with MS3110BDPC of the sensor with a titanium diaphragm.

### 3.3. Capacitance-to-voltage conversion circuitry using the MS3110

Stage 3 of the read-out circuitry involved the use of a die-type MS3110 IC chip that was manually integrated with a microfabricated capacitive pressure sensor. This

Table 2  
Measured data for two types of capacitive pressure sensors using the MS3110 with the MS3110BDPC

	Stainless steel	Titanium
Diaphragm radius (mm)	1	1
Diaphragm thickness ( $\mu\text{m}$ )	12.7	25.4
Gap ( $\mu\text{m}$ )	$\approx 27$	$\approx 37$
Back plate dimension (mm)	$3.5 \times 3.0$	$3.5 \times 3.0$
Applied pressure (kPa)	0–184	0–186
$\Delta V$ (V)	0.044	0.016
Sensitivity (mV/kPa)	0.238	0.0862

chip was the same IC as that which had been used in stage 2 with the MS3110BDPC evaluation board. The chip was first mounted on a glass substrate patterned with gold traces for its 17 pads to be used in wirebonding to the pressure sensors built on the stainless steel robust substrate. This was done separately because the substrate field around the sensor was coated with a thin film of SU-8 2 epoxy for insulation ( $\sim 6 \mu\text{m}$ ). This proved to be problematic during the wirebonding process because the ultrasonic technique used in the bonding process served to disturb and destroy adhesion of the epoxy layer on which the bonding pads for the chip were fabricated. By using a separate glass substrate for the IC, the integrity of the insulating epoxy layer was preserved during the wirebonding process. This can be easily connected in future process iterations.

In this stage, only the stainless steel diaphragm sensor was tested to demonstrate the integration of the robust

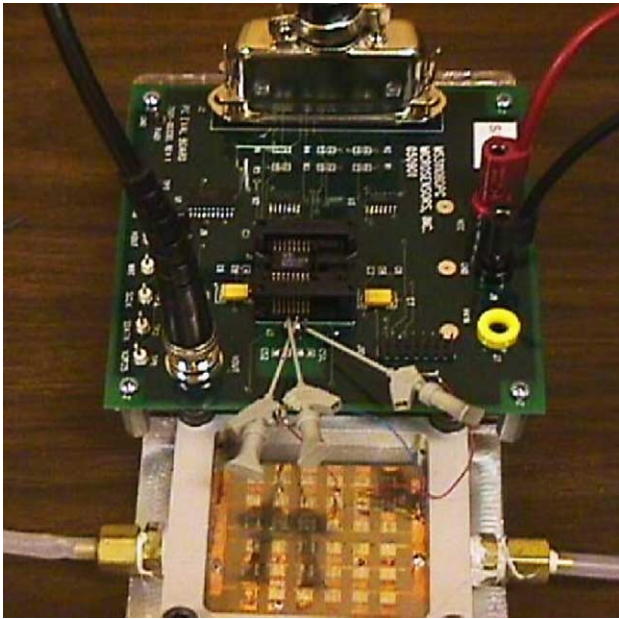


Fig. 13. The experimental test set-up using the MS3110 with the MS3110BDPC.

micromachined pressure sensor with a commercially available read-out IC. Fig. 14 shows the voltage output of the MS3110 for the stainless steel diaphragm sensor as a function of applied pressure from 0 to 75 kPa.

The measured value of relative voltage change is 2.85% over the applied pressure range from 0 to 75 kPa. This sensor contained a gap of 21  $\mu\text{m}$  and a sensitivity of 0.92 mV/kPa.

Fig. 15 shows the experimental test set-up used in evaluating the sensors using the MS3110. Fig. 16 shows a close-up of the MS3110 mounted on a glass substrate that has been

Voltage Change for stainless steel sensor with ASIC chip

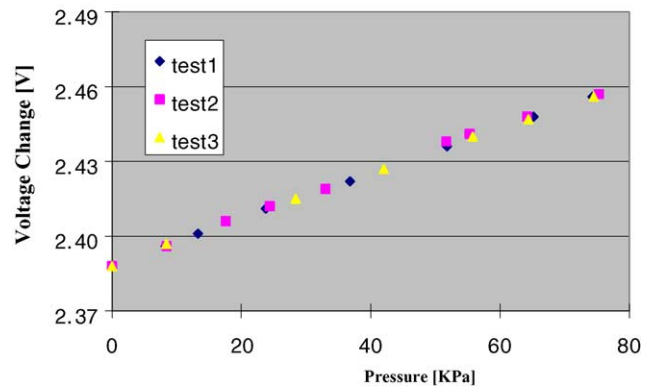


Fig. 14. The voltage output of the MS3110 for the stainless steel diaphragm sensor.

Table 3

Measured data for stainless steel diaphragm based on capacitive pressure sensors using the MS3110

	Stainless steel
Diaphragm radius (mm)	1
Diaphragm thickness ( $\mu\text{m}$ )	12.7
Gap ( $\mu\text{m}$ )	$\approx 21$
Back plate dimension (mm)	$3.5 \times 3.0$
Applied pressure (kPa)	0–75
$\Delta V$ (V)	0.068
Sensitivity (mV/kPa)	0.92

manually integrated on a stainless steel substrate with stainless steel diaphragm sensors.

The summarized data of the stainless steel diaphragm based on capacitive pressure sensors using the MS3110 are shown in Table 3.

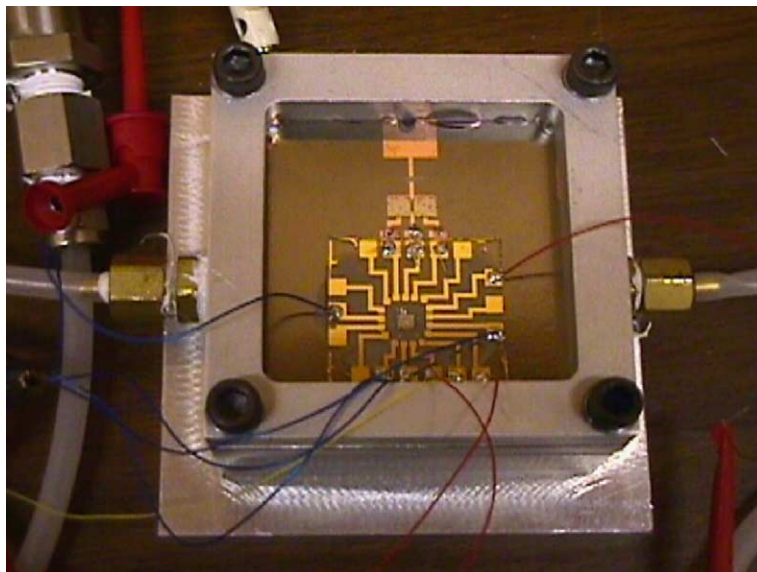


Fig. 15. The experimental test set-up used in evaluating the sensors using the MS3110.



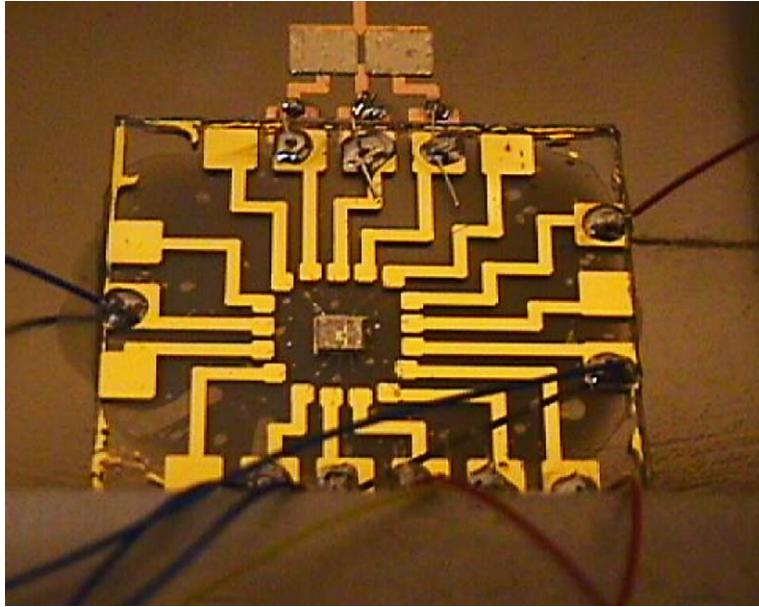


Fig. 16. A close-up of the MS3110 mounted on a glass substrate that has been manually integrated a stainless steel substrate with stainless steel diaphragm sensors.

#### 4. Conclusions

Stainless steel has been studied as a robust substrate material for micromachined devices in this paper. Lamination combined with traditional micromachining processes has been investigated as suitable fabrication methods for this robust substrate.

Three types of capacitive pressure sensors have been fabricated by using lamination processing with Kapton polyimide, stainless steel, and titanium films as diaphragms on the stainless steel shim stock substrate and demonstrated the integration with read-out circuitry on stainless steel substrate.

The goal of integrating the read-out circuitry to the sensors in this research is to demonstrate the way of integration circuitry to the sensors based on stainless steel substrate and is also to remove the parasitic capacitance due to the environmental noise.

In the final stage, the MS3110 IC in its un-packaged, die-type was integrated via wirebonding to the microfabricated sensors. The sensors showed that the performance of these sensors was affected much less the parasitics effects compared to the other two stages. The measured value of relative voltage change was 2.85% over the applied pressure range from 0 to 75 kPa. This sensor contained a gap of 21  $\mu\text{m}$  and had a sensitivity of 0.92 mV/kPa.

#### Acknowledgements

The support of the staff of the Microelectronics Research Center and GTRI Machine Shop at Georgia Tech is acknowledged. This work was supported by Defense Advanced Research Project Agency (DARPA) and the Air

Force Office of Scientific Research (AFOSR) under Contract F49620-97-1-0519.

#### References

- [1] H. Baltes, CMOS micro electro mechanical systems, *Sens. Mater.* 9 (6) (1997) 331–346.
- [2] N.C. MacDonald, SCREAM microelectromechanical systems, *Microelectron. Eng.* 32 (1/4) (1996) 49–73.
- [3] R.T. Howe, Applications of silicon micromachining to resonator fabrication, in: *Proceedings of the 1994 IEEE International Frequency Control Symposium (the 48th Annual Symposium)*, Cat. No. 94CH3446-2, 1994, pp. 2–7.
- [4] C.H. Mastrangelo, X. Zhang, W.C. Tang, Surface micromachined capacitive differential pressure sensor with lithographically-defined silicon diaphragm, in: *Proceedings of the International Solid-State Sensors and Actuators Conference-TRANSDUCERS'95*, vol. 1, 25–29 June 1995, pp. 612–615.
- [5] R.R. Tummala, *Fundamentals of Microsystems Packaging*, McGraw-Hill, New York, 2001.
- [6] Stein, et al., Thick film heaters made from dielectric tape bonded stainless steel substrates, in: *Proceedings of the ISHM '95*, Boston, MA, 1994, pp. 125–129.
- [7] G.T.A. Kovacs, *Micromachined Transducers Sourcebook*, McGraw-Hill, New York, 1998.
- [8] W.P. Eaton, J.H. Smith, Micromachined pressure sensors: review and recent developments, in: *Proceedings of the SPIE—The International Society for Optical Engineering*, vol. 3046, 1997, pp. 30–41.
- [9] A.S. Sedra, K.C. Smith, *Microelectronic Circuits*, CBS College Publishing, New York, 1982.
- [10] Y. Hsu, D. DeRoo, J. Murray, *Low Cost Sensor for Automotive Applications—The Fabless Strategy*, Microsensors Inc.

#### Biographies

*Sung-Pil Chang* received the BS degree in electronic engineering from Sung Kyun Kwan University, Korea in 1991. He received the MS and

PhD degree in electrical engineering from Georgia Institute of Technology in 1998 and 2002, respectively. Currently, he is working at the Photonics and MEMS group in Samsung Electro-Mechanics. His current research interests include Microsensors, RF MEMS and Optical MEMS.

*Mark G. Allen* received three bachelor degrees from the University of Pennsylvania in 1983: the BA in chemistry, the BSE in chemical engineering and the BSE in electrical engineering. Following this, he received the SM and PhD degrees in microelectronic materials from the Massachusetts Institute of Technology in 1986 and 1989, respectively.

He joined the faculty of Georgia Institute of Technology after a post-doctoral appointment at MIT. His work has received local, national, and international attention in both the popular press and in engineering trade publications. Specific research projects that have recently received media attention are: (1) magnetically actuated microrelays, smaller than a dime, that have potential use in automobile electronics, test equipment, and other areas where low actuation voltages are required; and (2) drug delivery via microneedles, tiny chips containing arrays of tiny needles, each thinner than a human hair, that can potentially be put on the skin for one-time injections and possibly left on the skin for continuous release of a medication under the control of a microprocessor.